Materials Science and Engineering B 159–160 (2009) 224–227

Contents lists available at ScienceDirect

Materials Science and Engineering B

journal homepage: www.elsevier.com/locate/mseb

Competitive iron gettering between internal gettering sites and boron implantation in CZ-silicon

M.I. Asghar*, M. Yli-Koski, H. Savin, A. Haarahiltunen, H. Talvitie, J. Sinkkonen

Helsinki University of Technology, P.O. Box 3500, FI-02015 TKK, Finland

ARTICLE INFO

Article history:
Received 5 May 2008
Received in revised form 11 November 2008
Accepted 22 December 2008

Keywords:
Iron
Silicon
Gettering
Boron
Ion implantation
Relaxation

ABSTRACT

Competitive gettering of iron was studied in silicon wafers with internal gettering sites in the bulk and implanted boron region near the wafer surface. The experimental results indicate that iron precipitation in the implanted boron region is significant. We show that internal gettering can reduce precipitated iron concentration in the heavily boron doped device layer but the optimization of internal gettering is a challenging task as typically precipitation (nucleation) is faster in heavily boron doped region. We also perform simulations to support the experimental results. Simulation results were found to be in accordance with the experimental results.

1. Introduction

In silicon technology, ion implantation is a standard process for doping and it can be used also for formation of gettering layer close to the active device layer. Benton et al. [1–3] have reported an extensive study of iron gettering by MeV boron, carbon and silicon implantation. In case of boron gettering can be modeled by combination of segregation of iron to boron doped layer and heterogeneous precipitation of iron to ion implantation damage [4].

Internal gettering (IG) is widely utilized in the integrated circuit industry to remove deleterious metal contaminants from the active region of the wafer to ameliorate device yields. It uses oxide precipitates and related defects to precipitate the metal impurities like iron, which hardly precipitate homogenously. However, it is clear that the existence of bulk defects does not automatically guarantee efficient gettering of iron. To achieve efficient internal gettering, iron precipitates must be nucleated at a sufficient number of bulk defects [5]. This nucleation strongly depends on the contamination level and processing temperature, i.e., supersaturation level of iron [6].

The above mentioned gettering techniques, IG and implantation gettering, occur simultaneously in many silicon devices, as areas of heavy doping which are part of any silicon-integrated circuit device, can provide efficient traps for metals and compete for impurities with intentionally introduced gettering sites. This is a concept of competitive gettering between gettering sites and devices [7]. In fact, while iron gettering by boron implantation is experimentally rather well studied [1–3], the studies of competitive gettering are not so comprehensive. In this work, we study competitive gettering of iron between implanted boron layer and internal gettering sites both experimentally and by simulations.

2. Experiments

The wafers used in the experiments were Czochralski grown boron doped silicon wafers. One set of wafers with thickness of 625 μm, have a resistivity of about 30 Ω cm and as grown oxygen content of 16 ppma (ASTM F 121-83 standard). The other set of wafers with thickness of 525 μm, have a resistivity of 21 Ω cm and as grown oxygen content of less than 8 ppma (ASTM F 121-83 standard). Wafers with high oxygen content (16 ppma) received different kinds of heat treatments for the formation of oxide precipitates\internal gettering sites and are labeled with 'B' in Table 1. Wafers with low oxygen content (<8 ppma) were used as a reference without intentional oxygen precipitation and are labeled with 'A' in Table 1. Then all of the wafers were intentionally contaminated with iron to a level of 1.7×10^{13} cm^{-3} by a procedure which is described in detail in Ref. [6].

After intentional contamination, wafers were implanted with a boron dose of 1×10^{15} cm^{-2} at an energy of 40 keV through the pad oxide thickness of 26.4 nm grown at 1000 °C. The implanted oxide was removed in diluted hydrofluoric acid (HF) solution. Then, the wafers were RCA cleaned including HF-dip as a last step. Implanted boron was activated by oxidizing at 1000 °C for 15 min, annealed at

* Corresponding author. Tel.: +358 44 2856 987; fax: +358 9 451 3195.
E-mail address: imran.asghar@tkk.fi (M.I. Asghar).

0921-5107/$ – see front matter © 2009 Elsevier B.V. All rights reserved.
doi:10.1016/j.mseb.2008.12.028

Table 1
List of samples. Heat treatment column shows the temperature and time of Hi–Lo–Hi oxygen precipitation processes. The values in the Table 1 are not experimentally measured. These values are used in the simulations to find an agreement between the simulation and experimental values. In simulations Defect zone in all the samples was 100 nm.

Sample	Heat treatment	Denuded zone width (μm)	Bulk defect density (cm^{-3})
B1	16 h @ 1150 °C + 2 h @ 550 °C + 16 h @ 1100 °C	70	1.5×10^8
B2	4 h @ 1150 °C + 6 h @ 650 °C + 16 h @ 1100 °C	50	4×10^8
B3	4 h @ 1150 °C + 2 h @ 650 °C + 16 h @ 1100 °C	50	1×10^8
B4	4 h @ 1150 °C	90	4×10^7
B5	16 h @ 1150 °C	100	7×10^7
A1	No heat treatment	Whole wafer	0

1000 °C for 25 min and cooled at the rate of 4 °C/min down to 800 °C before unloading the wafers from the furnace to room temperature.

After the room temperature step (RT), the wafers received a gettering anneal in N_2 ambient. The gettering anneal was performed at 700 °C for 1 h followed by cooling to room temperature. So-called "segregation anneal" was then performed at 450 °C for 1 h. The wafer loading and unloading between anneals to and from the room temperature are called consistently as RT step in this paper.

The iron content in implanted boron layer in each wafer was determined by etching the surface by a thickness of 2.4 μm using one-drop sandwich technique. The etching method was similar to the method presented in Ref. [8]. The etching solution residue was analyzed by total reflection X-ray fluorescence (TXRF) technique and the detection limit of measurement is about 3×10^{10} cm^{-2}, which was determined by measuring several clean reference wafers. The error estimate is 20% for determined iron content value in the boron layer.

3. Modeling

The cross section of silicon wafers under study can be divided into three parts: defect zone, denuded zone (DZ) and the bulk as shown in the Fig. 1. Defect zone is the ion implantation induced damage zone and is heavily doped by boron. Denuded zone (DZ) is the defect free zone between the ion implantation defects and the bulk defects. The bulk contains internal gettering (IG) sites. The internal gettering sites are characterized by the density of the defects (N_{bulk} = density of heterogeneous precipitation sites in bulk) and their radius (r_{bulk}). N_{bulk} and r_{bulk} for each wafer depend on the heat treatment given to the corresponding wafer. The width of the denuded zone depends on the temperature and time of the high temperature anneal. The density of defects in the defect zone (N_{ion} = density of heterogeneous precipitation sites in the implanted layer) and their sizes (r_{ion}) depend on the energy, dose and dopant activation anneal.

In this work, simulations are based on a model which takes into account both segregation of iron to boron doped layer and heterogeneous precipitation of iron to the implantation damage and internal gettering sites. The model uses an algorithm for diffusion and segregation of iron which is described in Ref. [9]. It takes into account both the effect of boron doping on iron solubility [10] and the effect of trapping of interstitially ionized iron by boron on iron diffusivity [11].

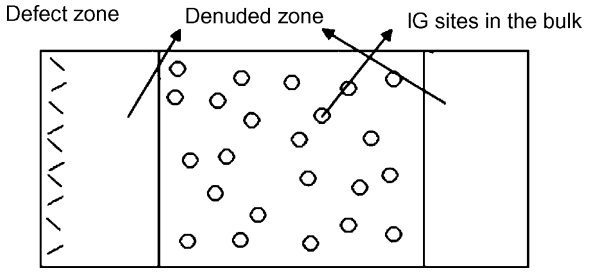

Fig. 1. The wafers structure. The implantation defect zone, denuded zone and the bulk containing IG sites.

Heterogeneous iron precipitation to ion implantation induced defects is simulated using a lumped model presented in Ref. [6,12]. Fokker–Planck equation (FPE) is used in the model to simulate the evolution of the size distribution of iron precipitates, given by:

$$\frac{\partial f(n,t)}{\partial t} = \frac{\partial}{\partial n}\left(-A(n,t)f(n,t) + B(n,t)\frac{\partial f(n,t)}{\partial n}\right) \quad (1)$$

where $f(n, t)$ is the density of heterogeneous precipitation sites containing n atoms of precipitated iron. A and B are given by:

$$A(n,t) = g(n,t) - d(n,t); \qquad B(n,t) = \frac{g(n,t) + d(n,t)}{2} \quad (2)$$

The growth and dissolution rates g and d are:

$$g(n,t) = 4\pi r_c D C_{Fe} \quad \text{and} \quad d(n,t) = 4\pi r_c D C_{Sol} \exp\left(\frac{E_a}{kTn^{1/2}}\right) \quad (3)$$

where r_c is the average capture radius of the iron precipitate, D is the diffusion constant of iron, C_{Fe} is the interstitial iron concentration, C_{sol} is the solubility of iron and factor $E_a/n^{1/2}$ describes the fact that iron has a higher chemical potential in a small cluster than in a large cluster.

The effect of boron doping on iron precipitation was taken into account by changes [4,13]:

$$C_{Sol}(B) = k_{Seg} C_{Sol} \quad \text{and} \quad D = D(B)$$

where K_{seg} is the segregation coefficient, $D(B)$ is the effective diffusion constant of iron, B is the boron concentration.

4. Results and discussion

The measured iron content (dense lines bars) in the front surface layer thickness of 2.4 μm for all the samples after the gettering anneals is shown in Fig. 2. The results show that the bulk defects (IG) decrease the iron concentration in the p+ layer. However, iron content in the p+ layer remains still relatively high, which we attribute to iron precipitation in the p+ layer.

The simulation results, without considering implantation defects, show the iron content only due to segregation effect (sparse lines bars in Fig. 2). The simulations show that iron concentration is above the detection limit only in the samples without IG sites if only segregation to p+ layer is taken into account. The experiments were designed based on these simulations i.e. assuming only segregation to p+ layer. The process RT-700 °C was chosen as the optimal gettering step based on the published results in Ref. [14]. The principal idea is very simple; during RT step (within ramps) iron nucleates to some of the bulk defects and during the following 700 °C anneal iron nuclei grow and thereby the dissolved iron concentration is decreased to the level of iron solubility at 700 °C, about 10^{12} cm^{-3}, in the bulk of the wafer. The second annealing step at 450 °C was designed only to "prove" that optimal gettering can prevent accumulation of iron into p+ layer simply because the dissolved (mobile) iron is captured by the bulk iron precipitates before the low temperature annealing. Note that a rather low temperature (450 °C)

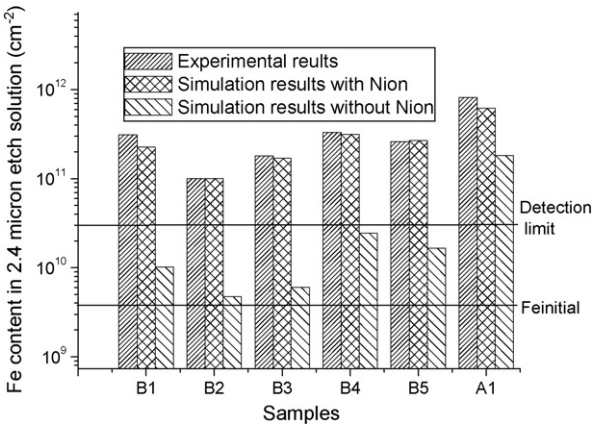

Fig. 2. Comparison of experimental and simulated values of Fe concentration in the device region. The dense lines bars are the experimental results, the cross lines bars and the sparse lines bars are the simulation results with and without considering implantation defects respectively. In simulations the sizes of ion implantation defects (r_{ion}) and bulk defects (r_{bulk}) were 15 nm and 40 nm respectively. Detection limit of measurements was 3×10^{10} cm^{-2}.

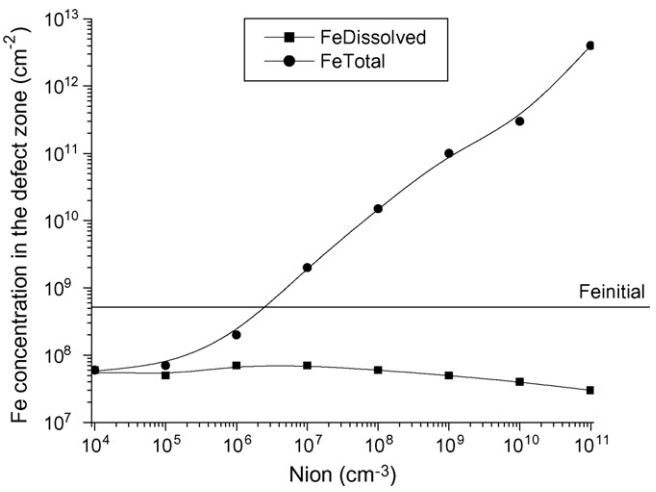

Fig. 3. Calculated Fe concentration in the 100 nm wide defect zone as a function of ion implantation defect density (N_{ion}). The precipitated Fe concentration is the difference of total and dissolved Fe concentration. Other parameters are as in Table 2.

was chosen to ensure sufficiently high segregation coefficient for reliable detection in samples without bulk defects.

The simulation results with considering implantation defects show iron content due to both segregation to p+ layer and precipitation in p+ layer (cross lines bars in Fig. 2). The difference in the results with and without considering implantation defects show that iron precipitation in p+ layer can explain the experimental results. The parameters $N_{ion} = 1 \times 10^{11}$ cm^{-3}, $r_{ion} = 15$ nm and the width of the defect layer of 0.1 μm were obtained by fitting the results without intentional oxygen precipitation. These parameters for p+ layer were used in simulations, when the parameters used for different oxygen precipitation profile corresponding to different pre-gettering heat treatments were adjusted to get agreement with the experimental results (Table 1). Thus, in simulations and most probably in experiments, the difference in results arises completely from the difference in density and size of the internal gettering sites in bulk. In all simulations of RT step a linear ramp rate of 100 °C/min was used.

The bulk defect densities used in the simulations are somewhat lower than the typical densities of oxide precipitates (≈total defect density in bulk) observed after high–low–high anneals (B1–B3 in Table 1). However, the values for the precipitate densities behave logically when considering the performed nucleation time and temperature (e.g. the density increases with annealing time). The defect densities in samples B4–B5 look also reasonable as the thermal history survived during the loading step could be easily in the order of 10^7–10^8 cm^{-3}.

In addition we performed some other simulations for the same process RT + 1 h @ 700 °C + RT + 1 h @ 450 °C. The nominal values used in the simulations are shown in the Table 2. We simulated process with a wide range of N_{ion} (Fig. 3). Fig. 3 shows that increasing ion implantation defects drastically increases the iron precipitation in the defect zone and above a cross-over point IG is unable to prevent iron accumulation to p+ layer. We simulated process also with a wide range of initial iron concentration (Fig. 4). Fig. 4 shows that increasing iron concentration above 1×10^{12} cm^{-3} increases the precipitation of iron in the defect zone. Both the experimental and simulation results indicate that removing iron totally from highly doped regions is very difficult due to iron precipitation in highly doped layers. When we optimize the thermal treatment in such a way that iron precipitates in the bulk, at the same time we enhance iron nucleation also in highly doped layers. Further, in some cases nucleation of iron is faster in highly doped regions than in low doped regions [13].

Then we may rise a question whether total iron concentration in highly doped region (device layer) is a good indicator for electrical characteristics of devices? If we extend our results to the case of a pn-junction, i.e., if we assume that in case of n+ layer the segregation and precipitation of iron is very similar than in case of p+ layer, we can give a very simple suggestion for optimal gettering. We propose

Table 2
Nominal values of the parameters used in the simulations for 1 h @ 700 °C + RT + 1 h @ 450 °C after the oxygen precipitation anneals.

Parameter	Values
Wafer thickness (μm)	625
Defect zone (μm)	0.1
Denuded zone (μm)	60
N_{bulk} (cm^{-3})	5×10^9
r_{bulk} (nm)	40
N_{ion} (cm^{-3})	1×10^{11}
r_{ion} (nm)	15
Boron dose (cm^{-2})	1×10^{15}
Ramp rate (°C/min)	100
$Fe_{initial}$ (cm^{-3})	1.7×10^{13}

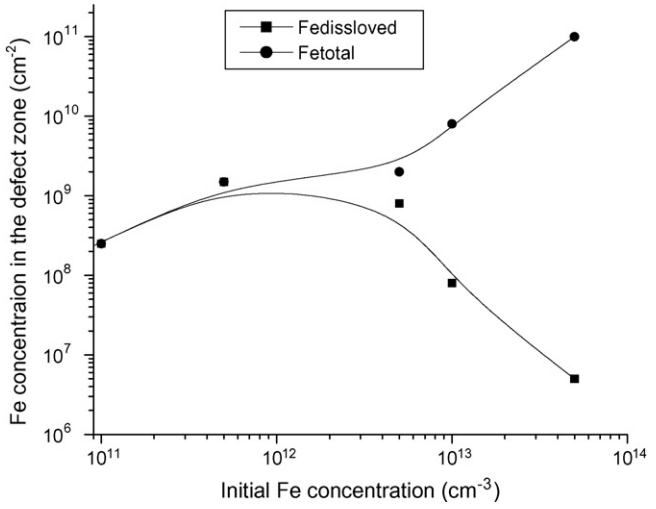

Fig. 4. Calculated Fe concentration in the 100 nm wide defect zone as a function of initial Fe concentration. The precipitated Fe concentration is the difference of total and dissolved Fe concentration. Other parameters are as in Table 2.

here that to optimize gettering, dissolved iron concentration in the depletion region of a junction has to be minimized. This can be done by highly doped regions if the iron precipitate density in highly doped regions is maximized in such a way that the average radius of iron precipitates is much smaller than the junction depth, i.e., the iron precipitate is not shunting the device. Note that in shallow junction devices this can be achieved only by decreasing the iron concentration (Fig. 4).

5. Conclusions

We have investigated competitive gettering of iron between the boron implantation layer and internal gettering sites in the bulk of the wafer. We have drawn the conclusion that iron concentration in the implantation region and in the bulk depends on both segregation and relaxation. In certain cases, internal gettering can reduce the iron concentration in the implantation region. However, optimization of internal gettering is a challenging task as optimization of the process in such a way that iron nucleates only in the bulk seems to be very difficult if not impossible.

Acknowledgements

The authors acknowledge the financial support from the Finnish National Technology Agency, Academy of Finland, Okmetic Oyj, Endeas Oy, Semilab Inc. and VTI Technologies Oy.

References

[1] J.L. Benton, P.A. Stolk, D.J. Eaglesham, D.C. Jacobson, J.Y. Cheng, J.M. Poate, N.T. Ha, T.E. Haynes, S.M. Myers, J. Appl. Phys. 80 (September (6)) (1996).
[2] P.A. Stolk, J.L. Benton, D.J. Eaglesham, D.C. Jacobson, J.Y. Cheng, J.M. Poate, S.M. Myers, T.E. Haynes, Appl. Phys. Lett. 68 (January (1)) (1996).
[3] J.L. Benton, P.A. Stolk, D.J. Eaglesham, D.C. Jacobson, J.Y. Cheng, J.M. Poate, S.M. Myers, T.E. Haynes, J. Electrochem. Soc. 143 (April (4)) (1996).
[4] A. Haarahiltunen, H. Talvitie, H. Savin, O. Anttila, M. Yli-Koski, M.I. Asghar, J. Sinkkonen, J. Mater, Sci.: Mater. Electron. 19 (2008) 41.
[5] A. Haarahiltunen, Doctoral Dissertation, Helsinki University of Technology, 2007.
[6] A. Haarahiltunen, H. Väinölä, O. Anttila, M. Yli-Koski, J. Sinkkonen, J. Appl. Phys. 101 (2007) 043507.
[7] A.A. Istratov, W. Huber, E.R. Weber, J. Electrochem. Soc. 150 (4) (2003) G244–G252.
[8] M.B. Shabani, T. Yoshimi, H. Abe, J. Electrochem. Soc. 143 (1996) 2025.
[9] H. Hieslmair, S. Balasubramanian, A.A. Istratov, E.R. Weber, Semicond. Sci. Technol. 16 (2001) 567.
[10] A.A. Istratov, W. Huber, E.R. Weber, J. Electrochem. Soc. 150 (2003) G244.
[11] H. Kohno, H. Hieslmaier, A.A. Istratov, E.R. Weber, Appl. Phys. Lett. 76 (2000) 2734.
[12] A. Haarahiltunen, H. Väinölä, O. Anttila, E. Saarnilehto, M. Yli-Koski, J. Storgårds, J. Sinkkonen, Appl. Phys. Lett. 87 (2005) 151908.
[13] A. Haarahiltunen, H. Talvitie, H. Savin, M. Yli-Koski, M.I. Asghar, J. Sinkkonen, Appl. Phys. Lett. 92 (2008) 021902.
[14] H. Väinölä, A. Haarahiltunen, M. Yli-Koski, E. Saarnilehto, J. Sinkkonen, Proceedings of the Electrochemical Society Fall 2004 Meeting, Honolulu, USA, 2004, p. 160.